

Supplementary Material

The Effects of Molecular Adsorption on Spin-wave Spectrum and Magnon Relaxation in Two-dimensional Cr₂Ge₂Te₆

Ke Wang¹, Kai Ren², Yuan Cheng³, Min Zhang¹, Hai Wang^{1*}, Gang Zhang^{3*}

¹ Xidian University, No. 2 Taibai Road, Xi'an, Shaanxi Province 710071, China

² School of Mechanical Engineering, Southeast University, Nanjing, Jiangsu 211189,
China.

³ Institute of High Performance Computing, A*STAR, Singapore 138632

Email: wanghai@mail.xidian.edu.cn; zhangg@ihpc.a-star.edu.sg

Part 1. Phonon spectrum and specific heat capacity

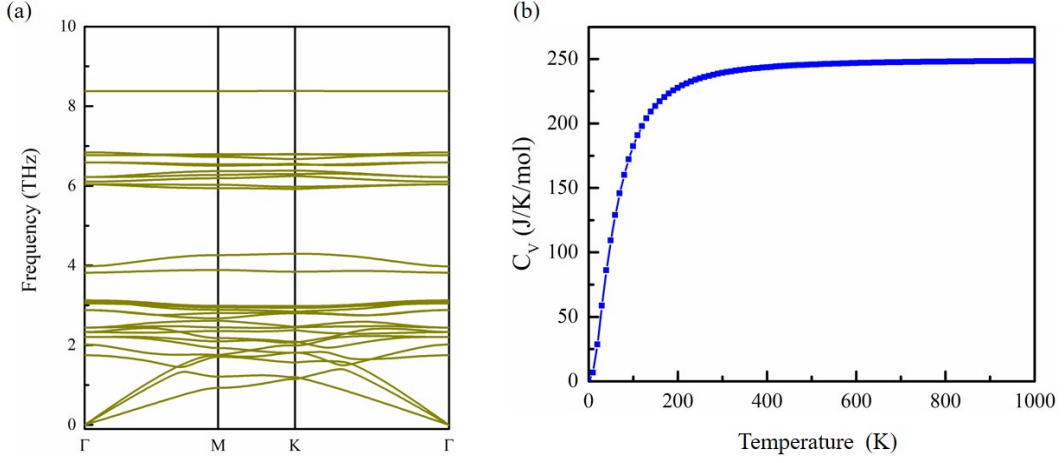


Figure S1. (a) Phonon spectrum and (b) the specific heat capacity versus temperature in $\text{Cr}_2\text{Ge}_2\text{Te}_6$ (CGT) monolayer.

The phonon spectrum of $\text{Cr}_2\text{Ge}_2\text{Te}_6$ (CGT) monolayer calculated by the Vienna *ab initio* simulation (VASP) package and PHONOPY code using density function perturbation theory (DFPT) is plotted in Figure S1(a). There is no imaginary frequency in phonon spectrum, revealing the thermodynamic stability of CGT monolayer. Meantime, it demonstrates the validation of specific heat capacity which is obtained simultaneously and presented in Figure S1(b). Then, we use the temperature dependence of specific heat capacity to calculate the Debye temperature Θ_D according to the Debye's T^3 -law

$$C_v = \frac{12\pi^4}{5} nk_B \left(\frac{T}{\Theta_D} \right)^3 \quad (\text{S1})$$

where n is the number of atoms, and k_B is the Boltzmann constant. The Debye temperature of monolayer CGT is ~ 243 K, which would be used in Debye model to determine the vibrational displacements of atom/molecule at finite temperature.

Part 2. Spin-wave spectrum based on Heisenberg model

In $2 \times 2 \times 1$ supercell, there are the nearest, next-nearest, and next-next-nearest exchange interactions. Here, only the nearest exchange interaction is highlighted, because the

next-nearest and next-next-nearest exchange interaction are much weaker¹. So we start from a nearest-neighbor (N) exchange Hamiltonian:

$$H = -\frac{1}{2} \sum_{\substack{l,f \in \text{Nearest} \\ l \neq f}} J_1 \mathbf{S}_l \cdot \mathbf{S}_f \quad (\text{S2})$$

where $\mathbf{S} = (S^x, S^y, S^z)$ is the spin vector of arbitrary magnetic lattice, its amplitude is S_0 , and J_1 is the exchange constant of the nearest-neighbor interaction. Due to the dependence of S^x , S^y , and S^z , transverse components $S^\pm = S^x \pm i S^y$ are defined.

According to Holstein-Primakoff (HP) approximation,^{2,3} S^\pm and S^z can be written as:

$$S^{a+} = \left(\sqrt{2S_0 - a^+ a}\right) a \approx \left(\sqrt{2S_0}\right) a, S^{a-} = \left(\sqrt{2S_0 - a^+ a}\right) a^+ \approx a^+ \left(\sqrt{2S_0}\right), S_a^z = (S_0 - a^+ a). \quad (\text{S3})$$

The Heisenberg Hamiltonian can be given as:

$$H = -J_1 \sum_{\substack{l,f \in \text{Nearest} \\ l \neq f}} \left[\frac{1}{2} (S_0 - a_l^+ a_l) (S_0 - a_f^+ a_f) + \frac{1}{4} (\sqrt{2S_0} a_l a_f^+ \sqrt{2S_0} + \sqrt{2S_0} a_l^+ a_f \sqrt{2S_0}) \right]. \quad (\text{S4})$$

Then, the coordinate space is transferred into reciprocal space by Fourier transform,

$$a_k = N^{-\frac{1}{2}} \sum_r e^{-ik \cdot r} a, \quad a_k^+ = N^{-\frac{1}{2}} \sum_r e^{ik \cdot r} a^+ \quad (\text{S5})$$

where \mathbf{k} is wave vector, \mathbf{r} is the position vector of magnetic lattice point, and N is the number of unit cell in supercell. The Hamiltonian in reciprocal space can be given by:

$$H = -J_1 \frac{1}{2} \sum_{\substack{l,f \in \text{Nearest} \\ l \neq f}} \left(S_0^2 - S_0 N^{(-1)} \sum_k (a_{l,k}^+ a_{l,k} + a_{f,k}^+ a_{f,k} - a_{f,k}^+ a_{l,k} \gamma_k - a_{l,k}^+ a_{f,k} \gamma_k) \right) \quad (\text{S6})$$

with structural factor $\gamma_k = \frac{1}{Z} \sum_{l,f \in \text{Nearest}} e^{ik \cdot (r_f - r_l)}$. Z is the coordination number for the nearest interaction. So the magnon frequency of system with single magnetic atom at k point can be written as:

$$\hbar \omega_k = J_1 Z S_0 (1 - \gamma_k). \quad (\text{S7})$$

There are two magnetic Cr atoms in the unit cell of CGT monolayer, thus there are acoustic and optical branches in spin-wave spectrum and Eq. (S7) should be updated as:

$$\hbar \omega_k^\pm = J_1 Z S_0 (1 \pm \gamma_k). \quad (\text{S8})$$

Here ‘+’ and ‘-’ denote the optical ($\hbar\omega_k^+$) and acoustic ($\hbar\omega_k^-$) branches of spin-wave spectrum, respectively.

Part 3. Mean-square displacements

The mean-square relative displacement σ_{ij} of atom pairs in crystal is defined as:

$$\sigma_{ij}^2 = \left\langle \left[(\mathbf{u}_i - \mathbf{u}_j) \cdot \mathbf{r}_{ij} \right]^2 \right\rangle \quad (\text{S9})$$

where \mathbf{u}_i is the thermal displacement of the i th atom from its equilibrium position and \mathbf{r}_{ij} is a vector pointing from the i th atom to the j th atom. The mean-square relative displacement can also be re-written as:

$$\sigma_{ij}^2 = \left\langle (\mathbf{u}_i \cdot \mathbf{r}_{ij})^2 \right\rangle + \left\langle (\mathbf{u}_j \cdot \mathbf{r}_{ij})^2 \right\rangle - 2 \left\langle (\mathbf{u}_i \cdot \mathbf{r}_{ij})(\mathbf{u}_j \cdot \mathbf{r}_{ij}) \right\rangle. \quad (\text{S10})$$

The first two terms are the mean-square displacements of the i th atom and the j th atom, while the third term represents the displacement correlation function. Using the phonon density of state (PDOS) and corresponding eigenvectors, σ_{ij} can be expressed as:⁴

$$\sigma_{ij}^2 = \frac{2\hbar}{NM} \sum_{\mathbf{k},s} \frac{(\mathbf{e}_{\mathbf{k},s} \cdot \mathbf{r}_{ij})^2}{\omega_{\mathbf{k},s}} \left[n(\omega_{\mathbf{k},s}) + \frac{1}{2} \right] (1 - \cos(\mathbf{k} \cdot \mathbf{r}_{ij})) \quad (\text{S11})$$

where N is the number of atoms, M is the mass of atom, $\mathbf{e}_{\mathbf{k},s}$ is the eigenvectors with wave vector \mathbf{k} for the s th phonon branch, $\omega_{\mathbf{k},s}$ is the phonon frequency, and

$n(\omega_{\mathbf{k},s}) = \frac{1}{e^{\hbar\omega_{\mathbf{k},s}/k_B T} - 1}$ is the phonon occupation number with reduced Plank constant \hbar

and Boltzmann constant k_B . It is clear the displacement of atom pairs not only depends on the mass of atom, but also relies on the distance of atom pairs. Eq. (S11) is equivalent to the more convenient integral expression:

$$\sigma_{ij}^2 = \int \frac{2\hbar}{M} \frac{\left[n(\omega) + \frac{1}{2} \right]}{\omega} \rho(\omega) d\omega \quad (\text{S12})$$

with the normalized and projected PDOS:⁵

$$\rho(\omega) = \sum_{\mathbf{k},s} (\mathbf{e}_{\mathbf{k},s} \cdot \mathbf{r}_{ij})^2 (1 - \cos(\mathbf{k} \cdot \mathbf{r}_{ij})) \delta(\omega - \omega_{\mathbf{k},s}). \quad (\text{S13})$$

To simplify Eq. (S12), we take a spherical average and neglect the difference between longitudinal and transverse phonon modes⁶. So $\rho(\omega)$ can be rewritten as:

$$\rho(\omega) = \frac{3\omega^2}{\omega_D^3} \left(1 - \frac{\sin(\omega r_{ij}/c)}{\omega r_{ij}} \right) \quad (\text{S14})$$

where c is the sound velocity, and ω_D is the Debye frequency. After integrating over ω , it can be obtained:

$$\begin{aligned} \sigma_{ij}^2 = & \frac{6\hbar^2}{Mk_B\Theta_D} \left(\frac{1}{4} + \left(\frac{T}{\Theta_D} \right)^2 \Phi_1 \right) - \frac{6\hbar^2}{Mk_B\Theta_D} \cdot \frac{1 - \cos(\omega_D r_{ij}/c)}{2(\omega_D r_{ij}/c)^2} \\ & - \frac{6\hbar^2}{Mk_B\Theta_D} \cdot \left(\frac{T}{\Theta_D} \right)^2 \cdot \int_0^{\Theta_D/T} \frac{\sin(\omega_D r_{ij} T x / c)}{(\omega_D r_{ij} T x / c)} \cdot \frac{x}{e^x - 1} dx \end{aligned} \quad (\text{S15})$$

where $\Phi_1 = \int_0^{\Theta_D/T} x/(e^x - 1) dx$. This equation is called ‘‘correlated Debye model’’^{5,7}. The

first term is the uncorrelated mean-square thermal displacement ($2\langle |\mathbf{u}_i|^2 \rangle$), and the last two terms represent the displacement correlation function (DCF). As demonstrated in the following, if the DCF can be ignored, the mean-square thermal displacement for one atom can be calculated by:

$$\langle |\mathbf{u}_i|^2 \rangle = \frac{3\hbar^2}{Mk_B\Theta_D} \left(\frac{1}{4} + \left(\frac{T}{\Theta_D} \right)^2 \int_0^{\Theta_D/T} \frac{x}{(e^x - 1)} dx \right). \quad (\text{S16})$$

Here, we calculated the mean-square relative displacements σ_{ij} of Cr, Ge, and Te atom pairs, and the results are shown in Figure S2(a). We can find the DCF has an impact on the mean-square relative displacement, and DCF relies on the mass of atom and the distance of atom pairs. For instance, the masses of Cr and Te are 52 and 127.6 amu while the distances of Cr atom pair and Te atom pair are 3.99 Å and 3.863 Å in CGT monolayer, which causes the DCF for Te atom is smaller than Cr. Meantime, the distance of Ge atom pair with mass of 72.6 amu is 6.91 Å, so that the DCF is close to zero. In order to describe the influence of DCF quantitatively, $\Delta\sigma_{ij}$ is defined as

$$\Delta\sigma_{ij} = \frac{\text{DCF}}{\left(2\langle|\mathbf{u}_i|^2\rangle\right)} \times 100\%. \quad (\text{S17})$$

The results are presented in Figure S2(b). It is obvious $\Delta\sigma_{ij}$ for Cr, Ge, and Te atoms in CGT monolayer are less than 10% in the temperature range of 0~60 K, revealing the DCF can be ignored in low temperature. Therefore, all of these atom displacement parameters used in our main text are calculated by Eq. (S16) without DCF, as in previous studies⁸⁻¹¹.

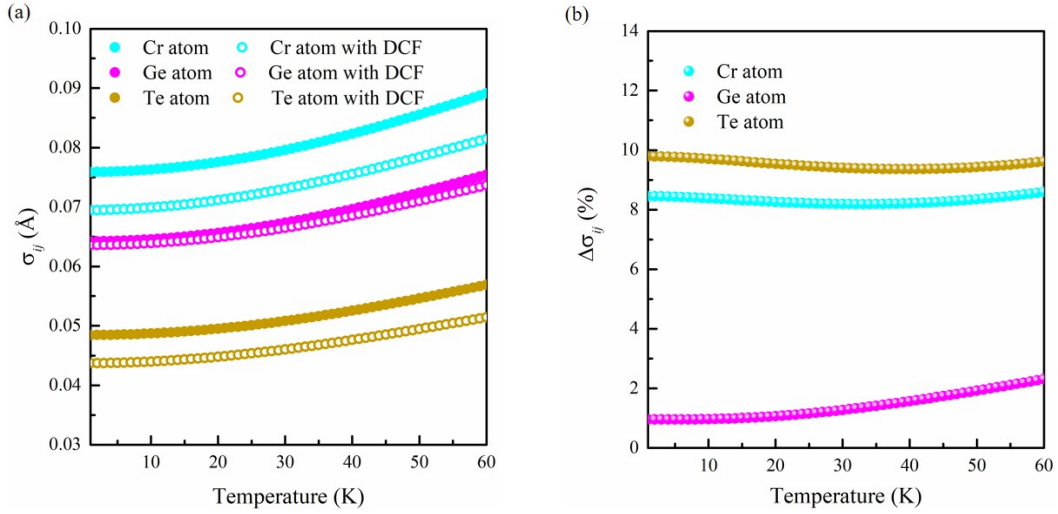


Figure S2. The mean-square relative displacements for Cr, Ge, and Te atoms (a), the difference between the mean-square relative displacements with and without displacement correlation function (b).

Part 4. Structural distortion and change in exchange constant

There are structural distortion and charge transfer in CGT monolayer with molecular adsorption, and we calculate the nearest exchange constant of CGT monolayer after adsorption by taking both distortion and charge transfer into consideration. To evaluate the structure distortion, we show the bond lengths of Ge-Ge, Ge-Te, and Te-Cr bonds in CGT monolayer before and after molecular adsorption in Table. S1. It is clear that the distortion caused by adsorption mainly occurs in the Ge-Ge bond, while the bond lengths of Ge-Te and Te-Cr bonds are almost unchanged.

Moreover, for separating the influence of distortion in CGT monolayer and charge transfer between molecule and substrate quantitatively, we replace the distorted CGT

substrate in NO_CGT system with pristine CGT monolayer, and calculate energies under different magnetic configurations (ferromagnetic and antiferromagnetic) and the nearest exchange constant J_1 , as shown in Table. S2. As shown in manuscript, the nearest exchange constant of pristine CGT monolayer is 6.87 meV. It is clear that the increase in J_1 due to charger transfer between molecule and substrate is 1.44 meV, and there is further increase of 0.82 meV if distortion in CGT sheet is taken into account. Thus the charge transfer between gas molecules and CGT substrate has larger impact on the nearest exchange constant of CGT monolayer.

Table. S1. The bond lengths of Ge-Ge, Ge-Te, and Te-Cr bonds in $\text{Cr}_2\text{Ge}_2\text{Te}_6$ (CGT) monolayer before and after molecular adsorption.

System Bond	NH ₃ _CGT	NO_CGT	NO ₂ _CGT	CGT
Ge-Ge	2.48 (Å)	2.47 (Å)	2.58 (Å)	2.42 (Å)
Ge-Te	2.64 (Å)	2.65 (Å)	2.63 (Å)	2.63 (Å)
Te-Cr	2.78 (Å)	2.77 (Å)	2.77 (Å)	2.78 (Å)

Table. S2. The energies under ferromagnetic (E_{FM}) and antiferromagnetic (E_{AFM}) configurations, and the nearest exchange constants J_1 of NO_CGT systems with distorted (NO_CGT) and pristine CGT (NO_Pre_CGT) monolayers.

System	E_{AFM} (eV)	E_{FM} (eV)	J_1 (meV)
NO_CGT	-213.031	-213.525	9.13
NO_Pre_CGT	-213.015	-213.464	8.31

References

- 1 Zhang, B., Hou, Y., Wang, Z. & Wu, R. First-principles studies of spin-phonon coupling in monolayer $\text{Cr}_2\text{Ge}_2\text{Te}_6$. *Phys. Rev. B* **100**, 224427 (2019).
- 2 Mead, L. R. & Papanicolaou, N. Holstein-Primakoff theory for many-body systems. *Phys. Rev. B* **28**, 1633 (1983).

- 3 Nieto, M. M. & Truax, D. R. Holstein-Primakoff/Bogoliubov Transformations and the Multiboson System. *Fortschr. Phys.* **45**, 145-156 (1997).
- 4 Jeong, I.-K., Heffner, R., Graf, M. & Billinge, S. Lattice dynamics and correlated atomic motion from the atomic pair distribution function. *Phys. Rev. B* **67**, 104301 (2003).
- 5 Sevillano, E., Meuth, H. & Rehr, J. Extended x-ray absorption fine structure Debye-Waller factors. I. Monatomic crystals. *Phys. Rev. B* **20**, 4908 (1979).
- 6 Debye, P. The Debye theory of specific heat. *Ann. Phys.(Leipzig)* **4**, 789-803 (1912).
- 7 Beni, G. & Platzman, P. Temperature and polarization dependence of extended x-ray absorption fine-structure spectra. *Phys. Rev. B* **14**, 1514 (1976).
- 8 Wang, L.-W., Xie, L.-S., Xu, P.-X. & Xia, K. First-principles study of magnon-phonon interactions in gadolinium iron garnet. *Phys. Rev. B* **101**, 165137 (2020).
- 9 Liu, Y., Xie, L.-S., Yuan, Z. & Xia, K. Magnon-phonon relaxation in yttrium iron garnet from first principles. *Phys. Rev. B* **96**, 174416 (2017).
- 10 Fischer, A. *et al.* Thermal and vibrational properties of thermoelectric ZnSb: Exploring the origin of low thermal conductivity. *Phys. Rev. B* **91**, 224309 (2015).
- 11 Maehrlein, S. F. *et al.* Dissecting spin-phonon equilibration in ferrimagnetic insulators by ultrafast lattice excitation. *Sci. Adv.* **4**, eaar5164 (2018).